

EXTERNALLY ILLUMINATED YOUNG STELLAR OBJECTS IN THE ORION NEBULA

John Bally¹, David Devine¹, and Ralph Sutherland²

Astrophysical, Planetary, and Atmospheric Sciences Department
University of Colorado, Boulder, CO 80309, USA

RESUMEN

Con el Telescopio Espacial Hubble se han detectado líneas de emisión intensas provenientes de los frentes de ionización que envuelven al gas denso residual de más de 50 objetos estelares jóvenes nacidos en la nube molecular de Orion en el último millón de años. En el centro de varias de esas envolventes se encuentran estrellas rodeadas por estructuras que podrían ser discos circumstelares observados en absorción contra el fondo nebuloso. En este artículo examinaremos los procesos físicos más importantes que deben tenerse en cuenta a la hora de estudiar la estructura y cinemática de esos objetos. También presentamos imágenes en el UV con resolución de siete unidades astronómicas de cinco entornos protoestelares iluminados externamente, así como la detección en esos objetos de emisión del hidrógeno molecular en $2.1218 \mu\text{m}$.

ABSTRACT

The Hubble Space Telescope (HST) has detected intense line emission from the ionization fronts that wrap around the residual dense gas surrounding over 50 YSOs born from the Orion Molecular cloud within the last 1 million years. Several of these envelopes have central stars surrounded by highly symmetric silhouettes that may be circumstellar disks seen in absorption against the nebular background. We will review the relevant physical processes that must be considered in evaluating the structure and kinematics of these objects. We also present 7 A.U. resolution UV images of 5 externally illuminated protostellar environments and report the detection of $2.1218 \mu\text{m}$ molecular hydrogen emission from these objects.

Key words: **STARS: PRE-MAIN-SEQUENCE — ISM: HII REGIONS — ISM: INDIVIDUAL (ORION NEBULA)**

1. INTRODUCTION

Stars are born from the gravitational collapse of dense molecular cloud cores. The Orion Nebula (M42), located at a distance of 470pc from the Sun, contains over 500 recently formed (mostly low-mass) stars that formed from the Orion A molecular cloud core within the past million years (Herbig & Tendirup 1986; Jones & Walker 1988). Dense neutral condensations (DNCs), many of which may contain young stellar objects (YSOs) that formed from the Orion molecular cloud have been “uncovered” within the last 10^5 years by the advancing HII region and now lie in the interior of the Orion Nebula (M42). The principle source of ionizing radiation in the region is the O6p star $\theta^1\text{C}$ in the Trapezium cluster and the O9 star $\theta^2\text{A Ori}$ located several arcminutes to the south.

The dense circumstellar environment from which low mass stars are being born is now lit up by the intense optical and UV radiation field of the massive O-stars, providing us with a powerful new means to investigate the

¹Center for Astrophysics and Space Astronomy (CASA)

²Joint Institute for Laboratory Astrophysics (JILA)

physics and structure of circumstellar and proto-planetary environments. The unprecedented angular resolution of the Hubble Space Telescope has now provided us with direct 7 A.U. resolution images of these DNC/YSOs.

Externally illuminated DNCs were first detected in the Orion Nebula by Laques & Vidal (1979) who found 7 compact knots bright in $H\alpha$ in the immediate vicinity of the Trapezium cluster. Free-free radio continuum from these objects and other sub-arcsecond diameter condensations was detected by the Very Large Array (VLA) radio telescope in the mid 1980s. (Churchwell 1987; Garay, Moran, & Reid 1987). Most such radio condensations coincide with the positions of stars in optical surveys of M42. Churchwell et al. (1987) suggested that the compact radio sources in the Orion Nebula may be externally ionized proto-planetary disks surrounding recently formed stars.

More detailed radio observations (Felli et al. 1993a,b) resulted in the discovery of over 30 compact free-free emitting sources. Some of these have been resolved and exhibit cometary tails pointing away from the Trapezium while others show arc-shaped emission facing the Trapezium. McCaughrean (1988) obtained high quality near-infrared images of the Trapezium region and demonstrated that nearly all compact VLA sources contain embedded stars.

O'Dell, Wen, & Hu (1993) and O'Dell & Wen (1994) detected intense line emission from ionization fronts that wrap around the residual dense gas that surrounds over 50 YSOs born from the Orion Molecular cloud. The HST observations support the model that identifies these objects as externally illuminated circumstellar environments.

O'Dell, Wen, & Hu coined the name *proplyd* (PROto PLANetarY Disk) to describe these objects, suggesting the internal structure of a forming star system rather than giving a simple external morphological description. This terminology joins the growing list of descriptive names assigned to compact nebulous objects, young stellar objects, and their environments. Another term used for similar objects is *PIG* (Partially Ionized Globule) which describes externally ionized neutral condensations embedded in HII regions. Thus a *PIG* may or may not be a *proplyd*. *PIGs* may be formed from *elephant trunks* which are externally ionized tongues of dense neutral gas that project into the ionized interior of HII regions. Herbig (1974) coined the term *interstellar teardrop* to describe the globules embedded in the Rosette nebula which have a shape very suggestive of the name. *EIDERS* (Externally Ionized Disks in the Environs of Radiation Sources) was coined to describe the VLA sources in Orion. *DEERS* (Deeply Embedded Energetic Radio Sources) describes YSOs that are still buried in the molecular cloud but visible at radio wavelengths by virtue of their free-free radio emission. *FOXES* (Fluctuating Optical and X-ray sourceS) describes more evolved YSOs which produce variable X-ray and non-thermal radio emission.

To consolidate this veritable zoo of objects we propose the following taxonomy, using a 2D classification scheme (see figure 1). On the horizontal axis we have the ambient optical/UV radiation field, ranging from completely obscured inside a dense Giant Molecular Cloud (GMC) up to to the intense field in the vicinity of massive O-stars. On the vertical axis we place the objects in order of decreasing gas content, or equivalently of increasing star formation evolution. Deep inside the GMC, on the upper left, dense self-gravitating *cores* form. In regions of high radiation, on the right, low density gas is ionized, exposing dense structures, at first observable as *elephant trunks* and then isolated *tear-drops* and finally globules or *PIGs*. *PIGs* refer to any isolated externally ionized clump, independent of whether or not it contains a star or disk. Thus the term *core* or *PIG* may also apply to more evolved objects, such as *proplyds*, based on external appearances. Subsequent vertical classification depends on the internal evolution of the *cores/PIGS*. When a rotationally supported disk forms they may be classified as *embedded disks* in the GMC interior, and *EIDERS* in the exposed ionized regions. Once a YSO forms inside an accretion disk, it emits radio, IR, and X-ray radiation powered by internal processes such as accretion flows. Now, the classification depends less on the external radiation field (indicated by the horizontal line extensions in the figure). We call very young sources where accretion and outflows produce radio emission *DEERS*. We call more evolved objects where the central star can be detected in some way *proplyds*. Finally, more evolved visible post T-Tauri stars where the extinction is low and which have active coronae that produce fluctuating non-thermal radio and X-ray emission are called *FOXES*. This description is meant to convey a broad picture of YSO evolution from an observers phenomenological point of view using terms such as *PIGs*, *DEER*, *EIDERS*, *proplyd*, and *FOXES* that have already been incorporated into the literature.

Many (and possibly most) young stellar objects may experience a phase in their evolution during which they are externally illuminated by intense ionizing radiation fields from nearby O-stars. For example, within the last 10^7 years more than 15,000 stars were formed from molecular clouds in the Solar vicinity (within 500 pc of the Sun). Of these about 5,000 to 10,000 have originated in the Orion, Perseus OB2, and Sco-Cen OB associations, and only between 500 to 1,000 have formed from dark clouds far away from O- and B-stars. Thus, most stars in the field are born in OB associations.

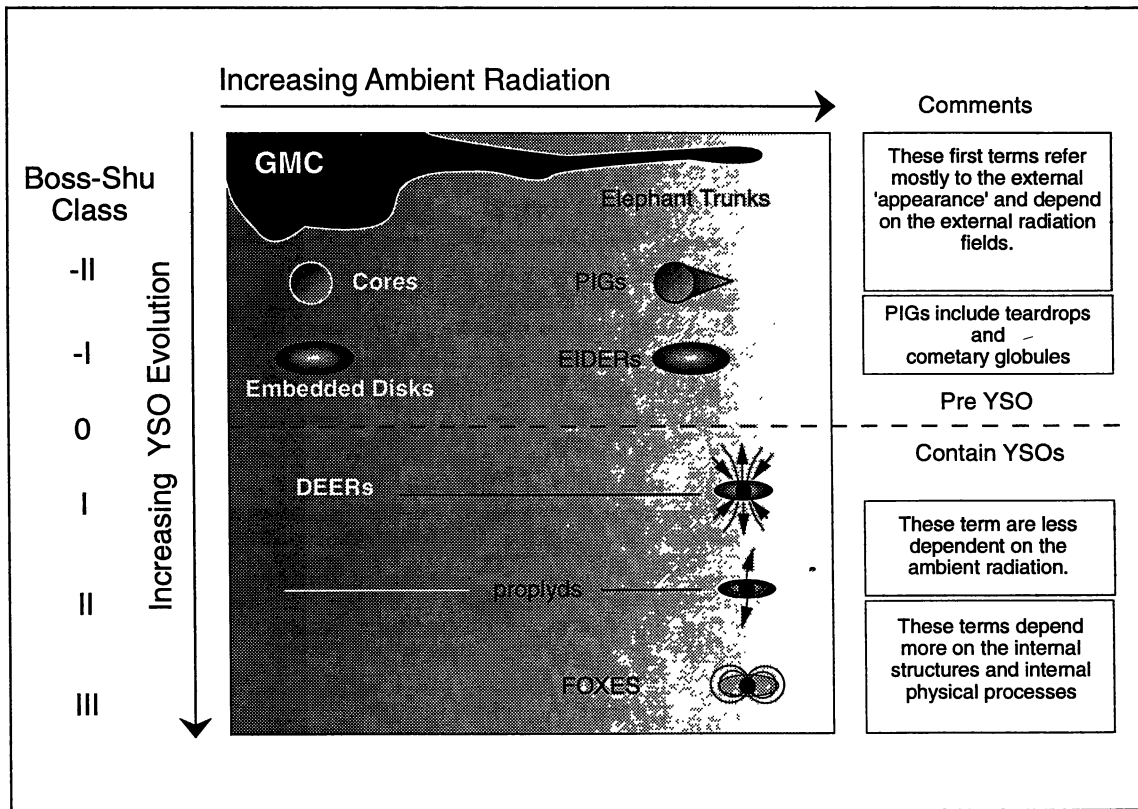


Fig. 1.– A Classification Scheme for proto- and young stellar gaseous structures.

In OB associations, most stars are formed in *transient clusters* similar to the those now observed in Orion (NGC2071, NGC2024, NGC2023, Trapezium, L1641N, and NGC1977). These clusters contain typically between 50 and 1,000 low mass stars, have extremely high initial central stellar densities (50,000 stars per cubic pc near the Trapezium), but dissolve within a few million years. In the Trapezium, the formation epoch was relatively brief ($< 10^6$ years) and has been brought to a halt by the birth of θ^1 C Orionis.

2. PROPERTIES OF EXTERNALLY ILLUMINATED CONDENSATIONS IN ORION

Externally illuminated DNCs in embedded in the Orion Nebula have the following properties:

- High intensity limb brightened photoionized edges seen in $H\alpha$, [NII], and [SII] that surround dense circumstellar YSO environments.
- Objects near θ^1 C Orionis (the brightest member of the Trapezium) exhibit long “cometary” tails pointing away from this star.
- Objects at larger distances from θ^1 C Orionis exhibit teardrop shapes with very short tails.
- Objects lying within a projected distance of $30''$ (0.07pc) of the Trapezium exhibit high excitation [OIII] arcs which may be shocks that wrap around the dense externally illuminated protostellar environment. The [OIII] arcs occur at a larger distance from the *proplyd* or *PIG* than the $H\alpha$, [NII], or [SII] photoionized emission, and are found in between the *proplyd* and the Trapezium stars.

- Nearly all of these nebular condensations contain low mass stars at their centers as seen in visual or near infrared wavelength images (McCaughrean 1988; McCaughrean & Stauffer 1994; Prosser et al. 1994; Stauffer et al. 1994). The location of the low mass stars in Orion on the H-R diagram indicates that most are less than 10^6 years old with a mean age of 3×10^5 years.
- Several objects contain opaque and dusty regions symmetric around the central star that may be disks seen in silhouette against the background nebular light.

Figures 2 and 3 show examples of externally illuminated YSOs embedded in the Orion Nebula. Figure 2 shows three images of five objects located roughly $10''$ west of θ^1 C Orionis. The three panels show the same roughly $6'' \times 6''$ field of view that contains the Laques & Vidal (1979) source LV4, LV5, LV6 (HST4), LV6N, and the Churchwell *et al.* (1987) source C26. (The large arc between LV6 and LV6N in the FOC image is an artifact.) The two smaller panels on the right show narrow-band $H\alpha$ and $[OIII]$ ($\lambda 5007\text{\AA}$) images of the field with a pixel size of $0.1''$ (47 A.U.). The vertical white streak is produced by charge bleeding from the bright star θ^1 A Orionis. Cometary tails point directly away from θ^1 C Orionis located to the left. The $[OIII]$ image shows arcs of high excitation gas wrapping around LV4 and LV5.

The left-hand panel of Figure 2 shows the same field of view but at a wavelength of $\lambda 2530\text{\AA}$ taken with the Faint Object Camera on HST through the F253M filter which transmits light in the semi-forbidden lines of $OII]$ and $CII]$ at $\lambda 2470\text{\AA}$ and $\lambda 2326\text{\AA}$. The pixel scale in this image is about $0.015''$ (7 A.U. at the distance of Orion). In the FOC image, all five objects show unresolved stellar images at the centers of the cometary condensations. LV6 and LV6N show dark regions surrounding their central stars within the bright arc-shaped ionization fronts which may be evidence for opaque and dusty circumstellar material.

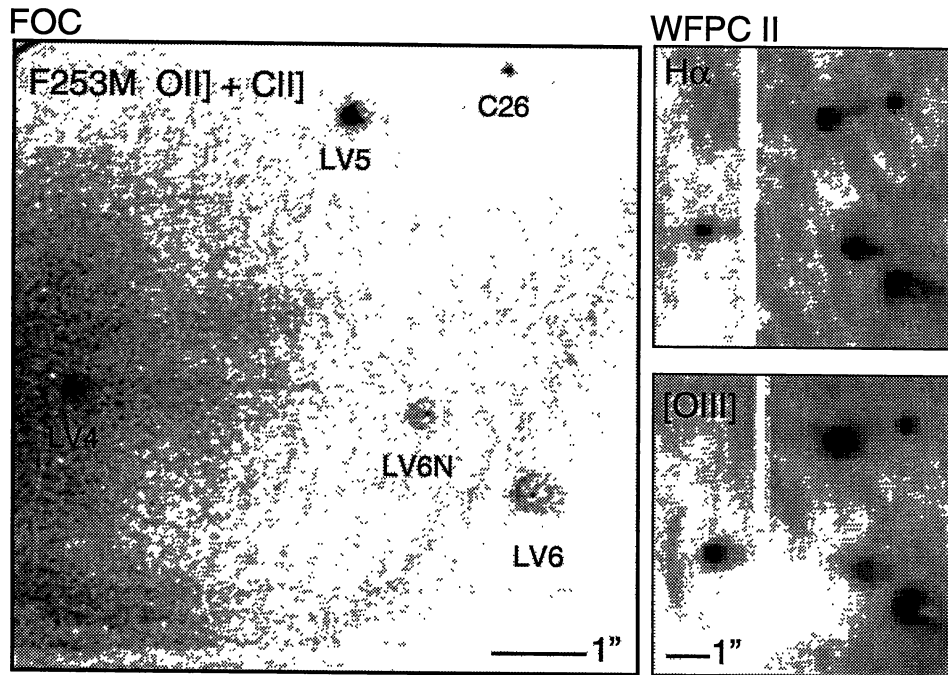


Fig. 2.— Externally illuminated proto-stellar environments $10''$ west of θ^1 C Ori.

Figure 3 shows narrow band $H\alpha$ and $[OIII]$ WFPCII images of HST10 located about $1'$ south of θ^1 C Orionis (taken from O'Dell & Wen 1994). Both images show a teardrop shaped nebular condensation centered on an elongated region of very high extinction. The ionization front surrounding the teardrop is brightest towards the side facing θ^1 C Orionis. The central dust lane may be completely opaque at visual wavelengths and perhaps even at near-infrared wavelengths. It may be a nearly edge-on disk that completely obscures the central star.

We detected $2.1218 \mu\text{m}$ wavelength H_2 emission from five out of eight externally illuminated YSO

environments using the high dispersion near-infrared spectrometer CSHELL on the IRTF on Mauna Kea on November 20 and 21, 1994. This instrument provides sufficiently high dispersion ($R = 40,000$) to resolve the H_2 line widths and to measure the radial velocity of the *proplyd* gas with respect to the background fluorescent nebular emission. The detected *PIGs* (most of which are *proplyds*) include HST 1, HST 8, HST 9, HST 10, and HST 17. In these objects, the detected emission clearly exceeds that from the background molecular cloud. The H_2 lines towards HST 4 (LV6) and HST 28 are only marginally stronger than the background, so our data can be considered to yield only a marginal detection. HST 16, which O'Dell & Wen (1994) argue lies completely outside the M42 Stromgren sphere (ionized region) in the foreground shows no evidence of H_2 emission. This object is seen only as a dark silhouette against the background nebula with no trace of photoionized edges and is therefore not a *PIG* (but is a *proplyd*). Therefore the UV radiation is too weak to either ionize the circumstellar gas or to excite H_2 emission.

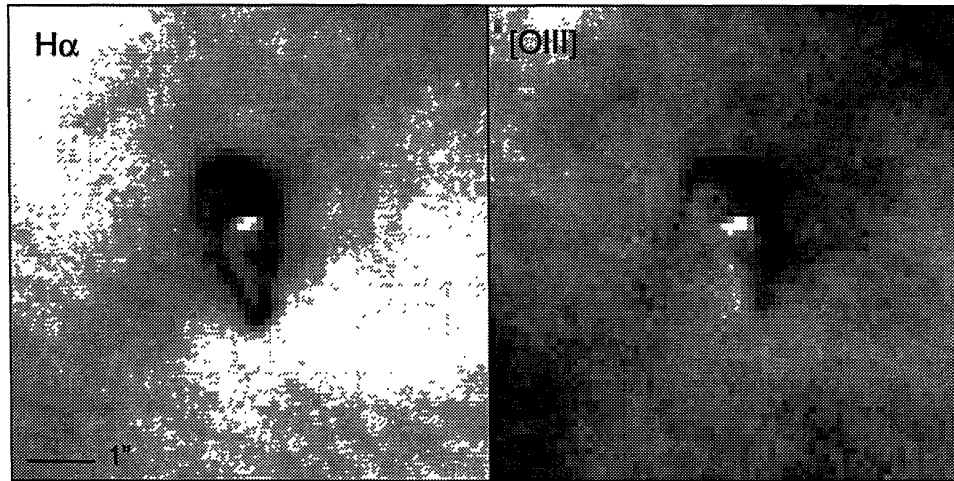


Fig. 3.— WFPCII images of HST10 located $1'$ southeast of the Trapezium.

The intensity of the H_2 emission can be explained by fluorescent excitation of the outer (molecular) layers of a dense externally illuminated circumstellar environment. The detection of the $2.1218\mu\text{m}$ S(1) line of H_2 demonstrates that molecular gas is present in large abundance in these envelopes. Furthermore, the line emission appears to be partially resolved in several objects, indicating line-widths of order 10 km/s, which suggests that gas motions are large. We do not know if this line width is due to orbital motion about the star, acceleration in the photo-evaporation zone, or turbulence. Further analysis of the velocity fields and the derivation of constraints on the excitation mechanism and molecular gas density will have to await full calibration of the data.

The large *PIG* HST 10 (see Figure 3) exhibits the strongest H_2 emission of all the objects we observed. Our H_2 S(1) line flux is consistent with all of the detected K-band ($2.2\mu\text{m}$) flux coming from H_2 line emission. McCaughrean (private communication) has searched for near-infrared continuum emission from the central star in HST 10. He fails to find a central star to a wavelength of about $3.6\mu\text{m}$. (Of all the Orion *PIGs*, HST 10 is the only object without firm evidence for a central star and hence is not a confirmed *proplyd* in our scheme.) This structure “looks like” an edge-on disk. Either HST 10’s disk is so opaque from our viewing angle that the central star is completely hidden ($N(\text{H}) > 10^{23}\text{ cm}^{-2}$) or HST 10 is simply an externally ionized globule without a central star. Millimeter or Sub-mm observations are needed to constrain the column density of HST 10.

3. PHYSICAL PROCESSES

Hot and massive stars ablate YSO environments by 3 mechanisms:

1. Mechanical ablation by the direct impact of a stellar wind or thermal evaporation by contact with the hot post-shock stellar wind bubble.

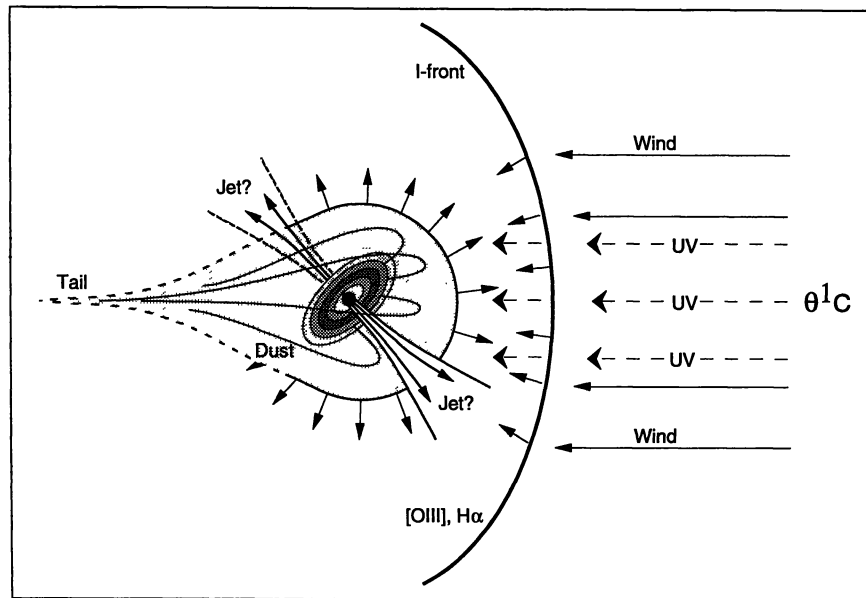


Fig. 4.— A model for externally illuminated YSO environments.

2. Photo-ablation by ionizing photons.
3. Radiation pressure acting on grains (which for a star like $\theta^1\text{C Ori}$ dominates all other forms of radial pressure by more than an order of magnitude).

Internal factors that affect the observed morphology include the evolutionary state of the YSO environment when first exposed to external UV irradiation. External factors which affect the morphology include the spectrum and strength of radiation field and the mechanical flux (in the form of gas flows) from the ionizing stars. Figure 4 shows a generic model of an externally illuminated YSO environment.

3.1. Evolutionary State and Mass of the YSO Environment

Star formation in an interstellar gas cloud is not coeval. Studies of star forming regions indicate that the duration of the star formation epoch can range from 10^5 to 10^6 years in a given cloud core to over 10^7 years for an entire giant molecular cloud spawning an OB association. Herbig & Tendirup (1986) and Jones & Walker (1988) have studied the age spread in the Trapezium cluster, finding few stars with evolutionary ages over 10^6 years, a median stellar age of 3×10^5 years, and some stars with ages as short as 10^5 years. Thus low mass (0.1 to $3M_{\odot}$) star formation has been proceeding for about 10^6 years in the OMC1 cloud core. We therefore expect an age spread for the YSOs embedded in M42. Furthermore, the evolution of more massive stars is likely to proceed faster than that of the lower mass members of the same cluster.

At the onset of nebular ionization (which presumably prevents further gravitational collapse and star formation from undifferentiated gas) YSOs in a variety of evolutionary stages will be exposed. The stages range from cloud cores on the verge of collapse [class -II or class -I in the Boss (1995) terminology], accreting proto-stars [class 0], to objects containing YSOs [classes I, II, and III in the Adams, Lada, & Shu (1987) terminology]. This sequence represents a progression of decreasing gas mass in the circumstellar environment.

3.2. Radiation

UV radiation interacts with the YSO environment by dissociating molecules, heating and ionizing the gas, and through radiation pressure acting on dust. The Lyman continuum luminosity of $\theta^1\text{C Orionis}$ is about $Q = 1.5 \times 10^{49}$ photons s^{-1} .

When the ionizing star first irradiates the YSO environment, an R-type ionization front moves

supersonically into the neutral gas. Recombinations between the resulting *PIG* and the ionizing star limit the progress of the ionization front when the mean density of the plasma at the ionization front is of order

$$n \approx (F/\alpha_B L)^{1/2} \approx 10^6 \text{ cm}^{-3}, \quad (1)$$

where $F = Q/4\pi d^2$ is the flux of Lyman continuum photons at a distance d from $\theta^1\text{C Orionis}$, (order $10^{14} \text{ cm}^{-2} \text{ s}^{-1}$ at $d = 10^{17} \text{ cm}$), $\alpha_B \approx 2.6 \times 10^{-13} \text{ cm}^3 \text{ s}^{-1}$ is the case B recombination coefficient for hydrogen, and $L \approx 10^{15} \text{ cm}$ is a characteristic dimension of an arc second sized *PIG* or *proplyd* in M42.

In the absence of dust, the location of the ionization front is determined by the recombination rate between the front and the hot star. However, in a dusty medium radiation pressure drives the dust away from the hot star back towards the YSO and its disk, forming a dust front and a cometary tail. The radiation pressure is roughly given by

$$\frac{P_{rad}}{k} \approx 8 \times 10^8 L_5 d_{17}^{-2} \quad (2)$$

where d_{17} is the distance from the star in units of 10^{17} cm , and k is Boltzmann's constant. A UV opaque dust-front forms in a layer where the gas-dust drift velocity nearly equals the velocity of heated and freshly ionized gas ablating off the face of the *proplyd* ($v = 3$ to 10 km/s). The ionized gas flowing away from the *proplyd* forms a low velocity "*proplyd* wind" with roughly an r^{-2} density profile and a mass loss rate

$$\dot{M} \approx \mu m_H n \pi r_p^2 c_{10} \approx 2 \times 10^{-7} r_{15}^2 c_{10} n_6 (M_\odot / \text{yr}), \quad (3)$$

where the wind velocity c_{10} is in units of 10 km s^{-1} (about the sound speed in the ionized gas), r_{15} is in units of 10^{15} cm (67 AU), and n_6 is the *proplyd* density in units of 10^6 cm^{-3} . The accumulation of dust in this layer where the inward dust drift is equal to the outward gas flow prevents the penetration of ionizing radiation into the interior of the *proplyd*, resulting in a sharp ionization zone just outside the dust front. Thus, the location of the ionization front is regulated by the opacity of the dust layer and therefore pinned near a value of 10^5 to 10^6 cm^{-3} by the gas-dust drift velocity. As further shown by Bertoldi & McKee (1990) the diffuse ionizing radiation field ($Q_{diff} \approx 1/6Q$) produces the characteristic teardrop shape.

3.3. Stellar Winds

$\theta^1\text{C Orionis}$ has a strong stellar wind with $M \approx 4 \times 10^{-7} M_\odot \text{ yr}^{-1}$ at a velocity of $v_w \approx 10^3 \text{ km s}^{-1}$ (Horwath & Prinja 1989) which drives a bubble into the surrounding medium. The wind bubble contains two zones (Weaver et al. 1977, Castor et al. 1975); an inner ram pressure dominated core surrounded by a hot bubble of shocked gas undergoing thermal expansion. The wind passes through a shock where the kinetic energy of motion is thermalized at

$$R_1 = 3 \times 10^{17} \dot{M}_{-7}^{3/10} n_3^{-3/10} v_3^{1/10} t_5^{2/5} (\text{cm}) \quad (4)$$

where \dot{M}_{-7} is the mass loss rate in units of $10^{-7} M_\odot \text{ yr}^{-1}$, n_3 is the undisturbed gas density outside the wind bubble in units of 10^3 cm^{-3} , v_3 is the wind velocity in 10^3 km s^{-1} , and t_5 is the age of the bubble in units of 10^5 years. The snowplow shock driven by the hot bubble into the surrounding undisturbed medium is located at a radius

$$R_2 = 3 \times 10^{18} \dot{M}_{-7}^{1/5} n_3^{-1/5} v_3^{2/5} t_5^{3/5} (\text{cm}) \quad (5)$$

The region between R_1 and R_2 is filled with a roughly isobaric hot ($> 10^6 \text{ K}$) gas. In the ram pressure dominated zone, the wind exerts a pressure (in units of K cm^{-3}) given by

$$\frac{P_w}{k} = \frac{\rho_w v_w^2}{k} = \frac{\dot{M} v_w}{4\pi k d^2} \approx 4 \times 10^7 \dot{M}_{-7} v_3 d_{17}^{-2} \quad (6)$$

The wind shock is expected to lie about $0.5'$ from the $\theta^1\text{C Orionis}$. *PIGs* and *proplyds* lying inside the ram pressure dominated region interact directly with the stellar wind, while those farther out are subject to thermal evaporation and turbulent stripping by the hot gas flowing outward in the thermalized wind bubble.

HST images in the [OIII] filter show arcs of emission lying between $\theta^1\text{C Ori}$ and many *proplyds* at about 10 to 30% of the *proplyd*/ $\theta^1\text{C Ori}$ distance. High dispersion spectra shows that in the central arc minute region of M42, the [OIII] emission exhibits high velocity wings with Doppler shifts in excess of 100 km s^{-1} . Therefore, this emission traces high velocity shocks. In Figure 5, we show three possible models for the [OIII] arcs.

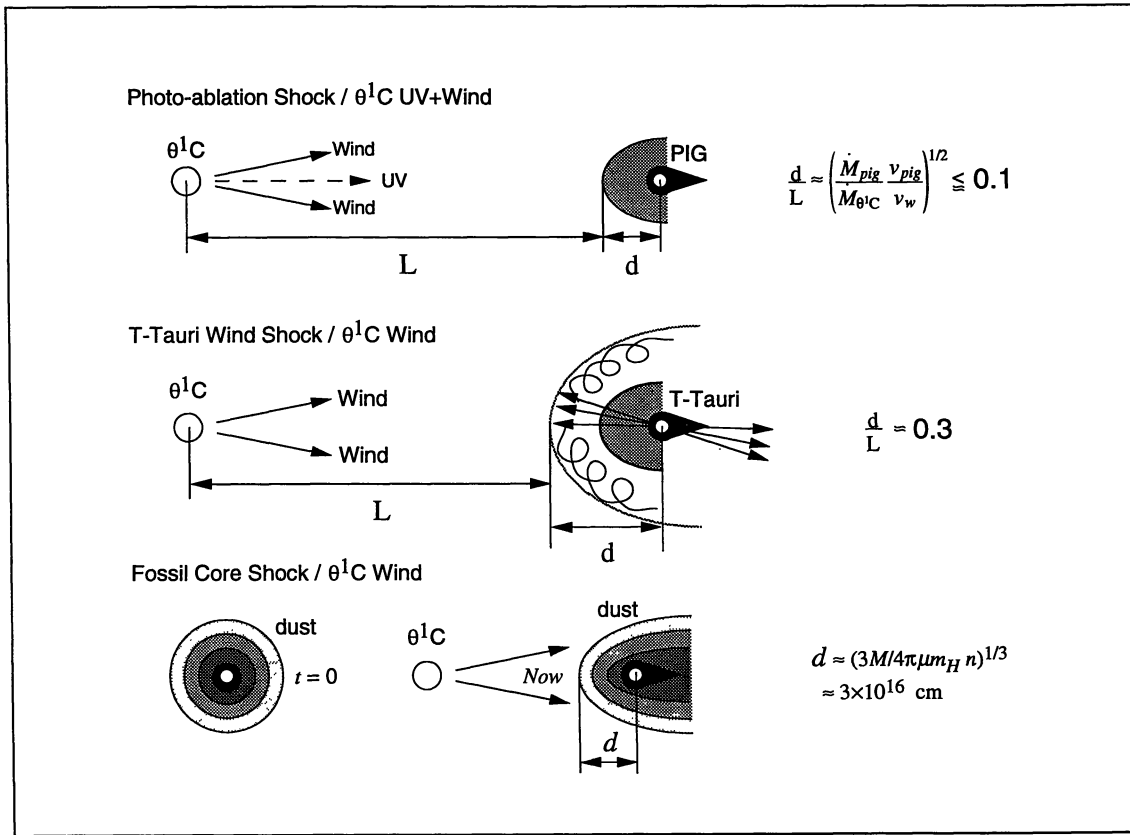


Fig. 5.— Three models for the [OIII] arcs.

In the top panel, the photo-ablated gas and the stellar wind from $\theta^1\text{C}$ Orionis interact where the ram pressures from the two flows are approximately equal. As in any two fluid system two shocks form; one propagating back into the photo-ablation flow, the other back into the stellar wind. Since the photo-ablation flow has a velocity close to the sound speed in ionized gas the shock propagating into this material is weak (or just a sound wave). The reverse shock propagating back into the stellar wind is strong and heats the inflowing material to temperatures of order $\mu m_H v_w^2/k \approx 10^7 \text{ K}$, but is rapidly advected by the ram pressure of the wind. Thus, this shock lies very close to the contact discontinuity formed between the *proplyd* ablation flow and the stellar wind, forming a bow that wraps around the PIG or *proplyd*. In this model, it is hard to understand the large observed separation between the *proplyds* and the [OIII] arcs since the mass loss rate due to photo-ablation given by equation 3 implies $d/L < 0.1$.

In the middle panel, the mass loss produced by a YSO wind (a jet or T-Tauri wind) blasts through the *proplyd* and interacts directly with the wind from $\theta^1\text{C}$ Orionis in a wind-wind collision. T-Tauri winds typically have $\dot{M} \approx 10^{-7}$ to $10^{-8} M_\odot \text{ yr}^{-1}$ at a wind velocity $v_{\text{T-Tauri}} \approx 200 \text{ km s}^{-1}$. For these parameters, the distance from the *proplyd* to the [OIII] arc is about $d/L \approx 0.3$ which is close to the observed location of the arcs.

In the lower panel, the dense neutral core (DNC) left over from the formation of the PIG or *proplyd* is photoionized and expands back into the HII region at roughly the sound speed, stalling when the mass has expanded to a point where it is in pressure equilibrium with its surroundings. Thus, the stellar wind shocks against the ionized density enhancement produced by the expanded *fossil DNC*. The ionized clump reaches a size of order $3 \times 10^{16} M_{\text{DNC}}^{1/3} n_5^{-1/3} \text{ cm}$, where M_{DNC} is the initial DNC mass (in units of M_\odot) and n_5 is the final electron density in units of 10^5 cm^{-3} . This is comparable to the radius of the [OIII] arcs. Again, the reverse shock is rapidly advected by the stellar wind ram pressure and therefore this shock is located close to the contact discontinuity. Charge exchange and collisional ionization en route to full ionization of oxygen may explain the brightness of the $\lambda 5007 \text{ \AA}$ line.

Hayward et al. (1994) found that the volume between the *proplyds* and the [OIII] arcs is bright at mid-infrared wavelengths near $12 \mu\text{m}$. It is possible that this emission (the so called *Ney-Allen Nebula*) traces dust

associated with the fossil cloud cores surrounding the *proplyds*. However, the amount of dust is very small (about 10^{-3} to 10^{-4} Earth masses). Given the large radiation pressure force, only a small fraction of dust is expected to remain in the fossil envelope; the rest has been blown away by the radiation pressure from θ^1 C Orionis as discussed above. Therefore, the Hayward et al. observations are consistent with the above models of *proplyd* evolution and both the wind-wind and fossil core models for the origin of the [OIII] arcs.

PIGs and *proplyds* lying at a greater distance than R_1 from θ^1 C Orionis will interact with hot gas in the wind bubble that is expanding at a velocity roughly given by \bar{R}_2 (equation 5). A *turbulent mixing layer* will form and strip gas from the ionized outer skin of the *proplyd* or PIG (Begelman & Fabian 1990; Slavin et al. 1993). Since the sound speed inside the hot bubble is larger than the bulk flow velocity, a bow shock does not form around the PIG or *proplyd*. However, in the turbulent mixing layer, where temperatures are between that of the bubble interior and the PIG or *proplyd* ionization front, the growth of shear instabilities may produce a complex of small scale weak shocks. In the absence of a strong and clearly defined shock, no [OIII] arcs are expected to form, and the photoionized gas traced by $H\alpha$ emission will mark the outer edge of the object.

This work was supported by NASA grant GO-5469.01-93A. RSS would like to acknowledge the support of the NASA Astrophysical Theory Program at the University of Colorado (grants NAGW-766 and NAGW-1479).

REFERENCES

- Adams, F. C., Lada, C. J., & Shu, F. H. 1987 ApJ, 312, 788
 Bertoldi, F., & McKee, C. 1990, ApJ, 354, 529
 Begelman, M. C., & Fabian, A. C. 1990, MNRAS, 244, 26B
 Boss, A. 1995, in Disks, Outflows and Star Formation, ed. S. Lizano & J. M. Torrelles, RevMexAASC, 1, 165
 Castor, J., McCray, R., & Weaver, R. 1975, ApJ, 200, L107
 Churchwell, E. B., Felli, M., Wood, D. O. S., & Massi, M. 1987, ApJ, 321, 516
 Felli, M., Churchwell, E. B., Wilson, T. L., & Taylor, G. B. 1993a, A&AS, 98, 137
 Felli, M., Taylor, G. B., Catarzi, M., Churchwell, & Kurtz, S. 1993b, A&AS, 101, 127
 Garay, G., Moran, J. M., & Reid, M. J. 1987, ApJ, 314, 535
 Hayward, T. L., Houck, J. R., & Miles, J. W. 1994, ApJ, 433, 157
 Herbig, G. H. 1974, PASP, 86, 604
 Herbig, G. H., & Tendrup, D. M. 1986, ApJ, 307, 609
 Horwath, I. D., & Prinja, R. K. 1989, ApJS, 69, 527.
 Jones, B. F., & Walker, M. F. 1988, AJ, 95, 1755
 Laques, P., & Vidal, J. L. 1979, A&A, 73, 97
 Mc Caughrean, M. J. 1988, PhD Thesis, University of Edinburgh
 Mc Caughrean, M. J., & Stauffer, J. R. 1994, AJ, 108, 1382
 O'Dell, C. R., Wen, Z., & Hu, X. 1993, ApJ, 410, 696
 O'Dell, C. R., & Wen, Z. 1994, ApJ, 436, 194
 Prosser, C. F., Stauffer, J. R., Hartmann, L., Soderblom, D. R., Jones, B. F., Werner, M. W., & McCaughrean, M. J. 1994, ApJ, 421, 517
 Slavin, J. D., Shull, J. M., & Begelman, M. C. 1993, ApJ, 407, 83
 Stauffer, J. R., Prosser, C. F., Hartmann, L., & McCaughrean, M. J. 1994, AJ, 108, 1375
 Weaver, R., McCray, R., Castor, J., Shapiro, P., & Moore, R. 1977, ApJ, 218, 377